

RESEARCH

Open Access



# Voltammetry in the spleen assesses real-time immunomodulatory norepinephrine release elicited by autonomic neurostimulation

Ibrahim T. Mughrabi<sup>1†</sup>, Michael Gerber<sup>1,2†</sup>, Naveen Jayaprakash<sup>1</sup>, Santhoshi P. Palandira<sup>1,4</sup>, Yousef Al-Abed<sup>1,2,4</sup>, Timir Datta-Chaudhuri<sup>1,2</sup>, Corey Smith<sup>3</sup>, Valentin A. Pavlov<sup>1,2,4</sup> and Stavros Zanos<sup>1,2,4\*</sup>

## Abstract

**Background** The noradrenergic innervation of the spleen is implicated in the autonomic control of inflammation and has been the target of neurostimulation therapies for inflammatory diseases. However, there is no real-time marker of its successful activation, which hinders the development of anti-inflammatory neurostimulation therapies and mechanistic studies in anti-inflammatory neural circuits.

**Methods** In mice, we performed fast-scan cyclic voltammetry (FSCV) in the spleen during intravenous injections of norepinephrine (NE), and during stimulation of the vagus, splanchnic, or splenic nerves. We defined the stimulus-elicited charge generated at the oxidation potential for NE (~0.88 V) as the “NE voltammetry signal” and quantified the dependence of the signal on NE dose and intensity of neurostimulation. We correlated the NE voltammetry signal with the anti-inflammatory effect of splenic nerve stimulation (SpNS) in a model of lipopolysaccharide- (LPS) induced endotoxemia, quantified as suppression of TNF release.

**Results** The NE voltammetry signal is proportional to the estimated peak NE blood concentration, with 0.1 µg/mL detection threshold. In response to SpNS, the signal increases within seconds, returns to baseline minutes later, and is blocked by interventions that deplete NE or inhibit NE release. The signal is elicited by efferent, but not afferent, electrical or optogenetic vagus nerve stimulation, and by splanchnic nerve stimulation. The magnitude of the signal during SpNS is inversely correlated with subsequent TNF suppression in endotoxemia and explains 40% of the variance in TNF measurements.

**Conclusions** FSCV in the spleen provides a marker for real-time monitoring of anti-inflammatory activation of the splenic innervation during autonomic stimulation.

**Keywords** Fast scan cyclic voltammetry, Spleen, Norepinephrine, Inflammation, Biomarker, Vagus nerve stimulation, Splanchnic nerve stimulation, Splenic nerve stimulation., Background

<sup>†</sup>Ibrahim T. Mughrabi and Michael Gerber have contributed equally to this work.

\*Correspondence:

Stavros Zanos  
szanos@northwell.edu

Full list of author information is available at the end of the article



## Background

The innervation of the spleen by the autonomic nervous system is implicated in the neural control of inflammation [1–3]. Both spinal sympathetic and vagal preganglionic neurons interact with the splenic nerve, and their stimulation results in increased splenic nerve activity and suppression of inflammation [4–12]. Part of this anti-inflammatory effect is initiated by the release of norepinephrine (NE) in the spleen parenchyma by terminals of the splenic nerve, followed by the release of acetylcholine by specialized T-cells and suppression of pro-inflammatory cytokine production by splenic macrophages. These findings prompted the development of new treatments for inflammatory diseases using neurostimulation devices to modulate the activity of autonomic nerves under the umbrella of the growing field of Bioelectronic Medicine [13]. Therapies involving cervical vagus nerve stimulation (VNS) [14], trans-auricular VNS [15, 16], splenic nerve stimulation [8], and ultrasound stimulation of the spleen [5, 6] all rely on the autonomic innervation of the spleen as the common final target to suppress inflammation in patients with inflammatory diseases [5, 6, 9, 11, 12].

As part of the clinical programming of anti-inflammatory bioelectronic therapies, parameters of neurostimulation need to be adjusted on an individual subject basis to maximize anti-inflammatory efficacy while minimizing off-target effects of neurostimulation [13, 17]. For example, stimulation of the cervical vagus nerve, which also innervates the larynx and the heart, can produce coughing or heart rate changes [18, 19], both undesired responses that could limit anti-inflammatory therapeutic efficacy. To deliver precision anti-inflammatory neuromodulation, the engagement of innervation of end-organs needs to be assessed, ideally in real time. Whereas markers for the engagement of autonomic innervation of the heart, lungs, and gut have been described [20, 21], no such marker exists for the spleen. A real-time marker for assessing the engagement of the innervation of the spleen in response to autonomic stimulation could contribute to safer, more effective, and precise anti-inflammatory bioelectronic therapies [13, 17]. Such a marker would also be helpful in mechanistic studies of neural reflexes activated by stimulation of autonomic nerves, something especially useful in rodent studies, in which direct recording of nerve activity evoked by stimulation is challenging because of small nerve size [21, 22].

To address this unmet need, we developed and evaluated a method to assess, in real time, the release of NE in the spleen in response to different forms of autonomic stimulation. The method is based on fast-scan cyclic voltammetry (FSCV), an electrochemical technique previously used to measure neurotransmitter release in the brain [23, 24] and recently suggested as a potential

marker for bioelectronic therapies [25, 26]. We defined a quantitative “NE voltammetry signal” as the total charge generated at the oxidative electrochemical potential for NE (~0.88 V) in response to a pharmacological or electrical stimulation intervention. We found that the NE voltammetry signal is dose responsive to injected NE and to electrical and optogenetic stimulation of autonomic nerves involved in the innervation of the spleen. The NE voltammetry signal is also responsive to pharmacologic or surgical manipulations that block the effect of neurostimulation on the innervation of the spleen. The magnitude of the NE voltammetry signal predicts the suppression of TNF release by nerve stimulation in acute inflammation, explaining about 40% of the variance in TNF values. Importantly, TNF suppression is greater at low values of the NE signal, and smaller at high values of the NE signal. Our findings indicate that voltammetry of the spleen is a feasible approach to assess, in real time, the engagement of the splenic innervation by different anti-inflammatory autonomic neurostimulation approaches.

## Methods

### Animals

Male and female C57BL/6 mice, ages 8–16 weeks, were purchased from Charles River Laboratories (Wilmington, MA). ChAT-IRES-Cre (#006410), Vglut2-IRES-Cre (#016963), Ai14 ROSA-tdTomato (#007914) and Ai32 ChR2-eYFP (#024109) mice were purchased from The Jackson Laboratory (Bar Harbor, ME) and crossed to produce ChAT-ChR2-eYFP, Vglut2-ChR2-eYFP, and ChAT-tdTomato mice used for optogenetic and splanchnic nerve stimulation experiments. Animals were housed using a 12-h light/dark cycle with ad libitum access to food and water. All animal procedures were approved by the Institutional Animal Care and Use Committee (IACUC) of the Feinstein Institutes for Medical Research, NY and complied with relevant NIH policies and guidelines.

### Surgical procedures

Following isoflurane anesthesia, induced at 4% and maintained at 1.5%, a 2-cm midline abdominal incision was made through the linea alba to just above the xyphoid process. The spleen was gently exposed by retracting the stomach and gut to the right while blunt dissecting the gastrosplenic ligament. The lower branch of the splenic neurovascular bundle was identified and gently dissected from surrounding fat. The spleen was then lifted out of the abdominal cavity and supported with cotton tips. A 34- $\mu$ m diameter carbon fiber microelectrode (Pinnacle Technology Inc, Lawrence, KS, USA) and an Ag/AgCl reference electrode were mounted on a stereotaxic

manipulator and inserted into the exposed spleen. The voltammetry electrodes were advanced ~0.5 mm into the diaphragmatic surface of the spleen opposite to the inferior branch of the splenic neurovascular bundle supplying the lower half of the spleen (Fig. 1a). To perform splenic nerve stimulation, the splenic neurovascular bundle was placed into a bipolar micro-cuff electrode to deliver electrical stimulation to the splenic nerve, which runs along the splenic artery. To isolate the left cervical vagus nerve, a 1-cm midline incision was made in the anterior neck and the salivary glands were retracted laterally along with the sternocleidomastoid muscle. The

vagus nerve was then identified within the carotid sheath, dissected away from connective tissue, and gently placed on a bipolar micro-cuff electrode for electrical stimulation or a custom-made optical cuff for optogenetic stimulation. To perform left splanchnic nerve stimulation, ChAT–tdTomato mice were used to correctly identify the nerve as it enters the celiac–superior mesenteric (CSM) ganglion complex using a fluorescence dissecting microscope. Mice were anesthetized and underwent a midline abdominal incision. The intestines were gently retracted to the right and covered with gauze saturated with warm saline. The celiac artery was then identified, and the left

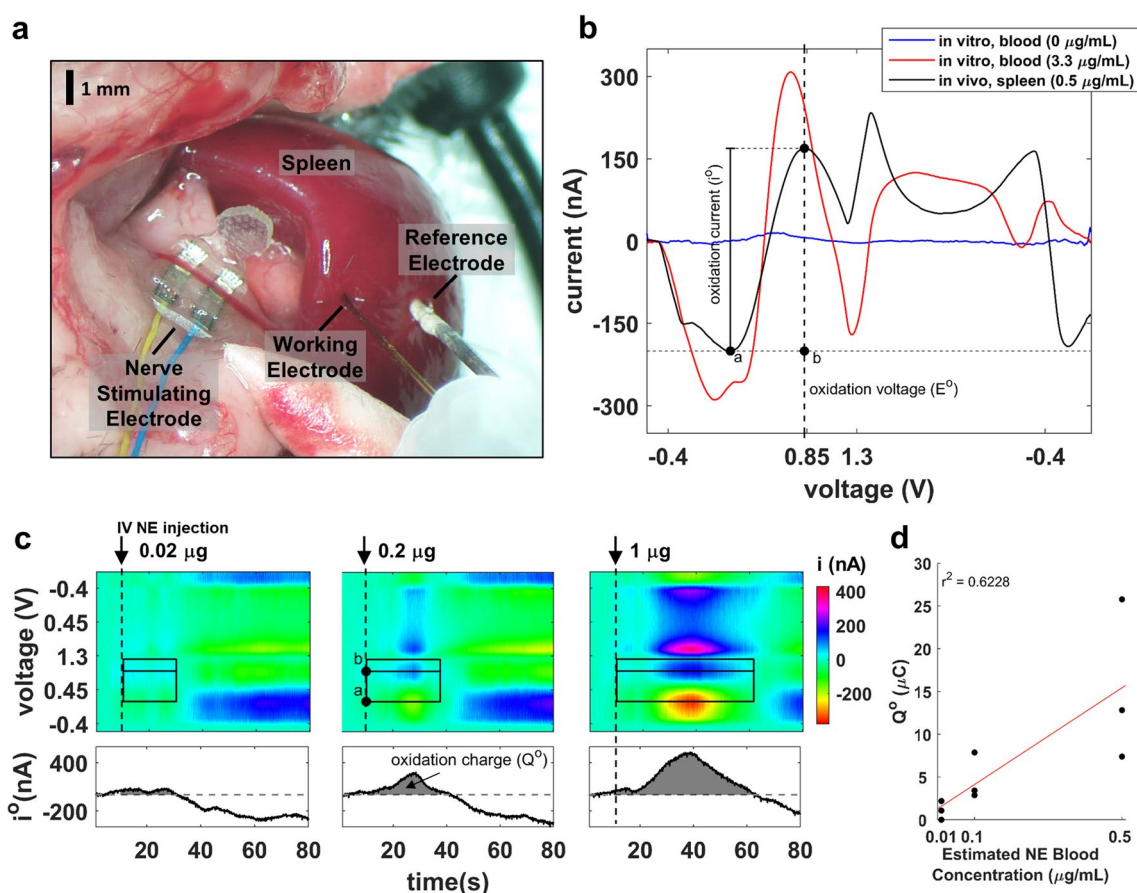


**Fig. 1** Spleen voltammetry signal responsive to changes in NE. **a** Carbon fiber working electrode and a reference electrode are inserted in the spleen for recording fast scan cyclic voltammetry. A bipolar electrode is placed on the splenic neurovascular bundle for splenic nerve stimulation; in other experiments, the stimulating electrode is placed on the cervical vagus nerve or the splanchnic nerve. **b** Averaged cyclic voltammograms during voltage sweeps (–0.4 V to 1.3 V and back to –0.4 V) in vitro (in heparinized blood, 0 and 3.3 μg/mL NE) and in vivo (in live spleen, 0.5 μg/mL est. peak blood NE concentration); the vertical dotted line denotes the NE oxidation voltage ( $E^0$ ), and the calculation of oxidation current ( $i^0$ ) is represented. **c** Representative time-resolved voltammograms during intravenous bolus injection of NE (100 μL). Top panels: current amplitude (represented by color) at different values of sweeping voltage (ordinate), at different times relative to NE injection (abscissa). Outer black box represents the voltage and time boundaries of the peak oxidation current signal (outer boundaries); horizontal line inside box marks the oxidation potential for NE. Dashed vertical line denotes time of drug administration. Bottom panels: time-course of oxidation current, calculated as shown in **b**, during the same time period. Grey-shaded area under the  $i^0$  trace represents the total oxidation charge ( $Q^0$ ) generated within the time boundaries indicated in the top panels. **d**  $Q^0$  at multiple NE concentrations measured in 3 animals, at different estimated NE concentrations. Solid line represents linear fit; Pearson’s  $r = 0.79$ ,  $p = 0.01$

CSM ganglion complex was located around its origin marked by bright red fluorescence. The left splanchnic nerve was traced from the upper left edge of the ganglion back to its thoracic para-vertebral level. The nerve was cuffed with a bipolar electrode (Flex, Feinstein Institutes, described in [27]) to deliver electrical stimulation.

#### Fast-scan cyclic voltammetry

A two-electrode commercial system (Pinnacle Technology Inc) was used to perform FSCV using a triangular waveform scanning from  $-0.4$  to  $1.3$  to  $-0.4$  V at  $400$  V/s with a cycling frequency of  $10$  Hz and  $-0.4$  V holding potential between cycles. The commercial  $34$   $\mu\text{m}$ -diameter carbon fiber electrodes (Pinnacle Technology Inc) are enclosed in a silica sheath and extend  $0.5$  mm beyond the edge of the sheath. The carbon fiber electrodes were reused for multiple experiments after cleaning by soaking in enzymatic instrument cleaner (Roboz, Gaithersburg, MD, USA) for  $15$  min to remove biological fouling, then rinsing with water. Before each experiment, the electrodes were tested by examining the background current for any shifts in shape or magnitude [28]. Electrodes that exhibit increased background current or shifts in shape were discarded. Current and voltage data were acquired using the continuous scanning mode at a sampling rate of  $1000$  Hz. For *in vitro* experiments, blood was collected by cardiac puncture using a heparin-flushed syringe and then pooled together (about  $5$  mL) before aliquoting into a 96-well plate ( $300$   $\mu\text{L}$  per well). Freshly made NE in PBS solution was added to each well, filled with either PBS or blood, to achieve a final concentration of  $0$ ,  $0.33$ , and  $3.3$   $\mu\text{g}/\text{mL}$ . After recording background current from the vehicle-treated well, NE was probed in the remaining wells. For *in vivo* experiments, after inserting the voltammetry electrodes into the spleen, the working electrode was conditioned for about  $10$  min before collecting voltammetry data, over which time baseline was typically stable.

#### Intravenous infusions

To establish an intravenous (IV) line, the right external jugular vein was isolated and ligated distally while blocking blood flow with a loose suture proximally to prevent bleeding. A small incision was then made between the two sutures and a 1-French catheter (Instech Labs, Plymouth Meeting, PA, USA) was advanced into the vessel followed by a  $50$   $\mu\text{L}$  saline bolus to confirm patency. In some experiments,  $100$   $\mu\text{L}$  NE bitartrate (SAGENT Pharmaceutical, Schaumburg, IL, USA) boluses were administered sequentially at escalating doses ( $0.2$   $\mu\text{g}/\text{mL}$ ,  $2$   $\mu\text{g}/\text{mL}$ ,  $10$   $\mu\text{g}/\text{mL}$ )  $10$  min apart. The final concentration of circulating NE after each dose was estimated for an average mouse weight of  $25$  g based on a volume of

distribution of  $2$  mL estimated to be the total blood volume in a mouse [29]. All IV injections were prepared in saline and administered as  $100$   $\mu\text{L}$  bolus injections over  $10$  s.

#### Nerve stimulation

Electrical stimulation was delivered using commercial bipolar micro-cuff electrodes (CorTec, Freiburg, Germany) or custom-made flexible electrodes (Flex) made in-house [27], connected to a stimulus generator (STG4008, Multichannel Systems, Reutlingen, BW Germany). Stimulus trains consisted of bi-phasic charge-balanced square pulses of  $10$  s duration,  $500$   $\mu\text{s}$  pulse width (PW), and  $10$  Hz frequency at varying intensities. In some experiments, the splenic nerve was blocked by applying a piece of gauze saturated with  $2\%$  lidocaine on the splenic neurovascular bundle for  $10$  min. In cervical vagotomy experiments, the vagus nerve was mechanically stabilized on the micro-cuff electrode by applying a drop of two-component silicone (Kwik-Sil, World Precision Instruments, Sarasota, FL, USA) and then sectioned either proximal or distal to the cuff. For optogenetic stimulation experiments, a custom-made optical cuff, consisting of a blue LED light (XLAMP XQ-E, Cree LED, Durham, NC, USA) integrated into a molded silicone cuff, was connected to a stimulus generator (MCS) operating in voltage mode. Optical stimulation was delivered using  $10$ -s stimulus trains of  $10$  ms PW and  $30$  Hz frequency while varying intensity by changing the voltage driving the LED. During vagus stimulation experiments, animals were instrumented with ECG leads and nasal airflow temperature sensors to monitor heart rate and breathing rate responses.

#### Norepinephrine depletion

Reserpine in DMSO (Tocris Bioscience, Bristol, UK) was diluted in saline and administered to animals by *i.p.* injection ( $5$  mg/kg).  $18$ – $24$  h post-injection, NE elicited by SpNS was probed using voltammetry in the spleen as described.

#### Endotoxemia model

Following isoflurane anesthesia, the spleen was exposed through a  $1$ -cm lateral abdominal incision just below the left costal margin and instrumented with voltammetry electrodes as described before. After  $10$  min of electrode conditioning, the splenic neurovascular bundle was electrically stimulated for  $3$  min ( $300$ – $500$   $\mu\text{A}$ ,  $500$   $\mu\text{s}$ ,  $10$  Hz) using a bi-polar cuff electrode (CorTec) while performing spleen FSCV. To ensure complete recording of the elicited NE signal, FSCV sweeping was continued for at least  $10$  min post-stimulation and the disappearance of the signal was

verified before stopping the recording. The voltammetry electrodes were then carefully removed, and the micro-puncture site was repaired with tissue glue. The abdominal incision was closed in two layers, and the animal was allowed to recover from anesthesia. Two hours post-stimulation, animals were injected intraperitoneally with 1 mg/kg of lipopolysaccharide (LPS endotoxin from *E. coli* 0111:B4 ultra-pure; InvivoGen, San Diego, CA, USA) dissolved in saline. Heparinized blood was collected by cardiac puncture under terminal anesthesia 90 min post-LPS injection and centrifuged immediately at  $2000\times g$  for 10 min. Plasma TNF- $\alpha$  was determined using TNF- $\alpha$  ELISA kit (Cat # 88-7324-88, Invitrogen, Waltham, MA, USA) following manufacturer's instructions.

#### Data analysis and statistics

Voltammograms were background-subtracted and smoothed with a moving average filter of 5 ms. Oxidation current ( $i^o$ ) was determined in each voltammetry cycle as the difference between the trough and the peak of the current trace during the oxidation part of the cycle (points a and b, respectively, Fig. 1b). The "NE voltammetry signal" was defined as the integral of  $i^o$  over time during an integration window, corresponding to the total oxidation charge ( $Q^o$ ) (Fig. 1c). This method was chosen, because peak and duration of the NE transient in response to a stimulus are both likely to be important for downstream biological effects of NE release. The  $i^o$  integration window was determined by an algorithm that calculates the time at which the  $i^o$  trace rises, then returns to baseline. The algorithm for determining the window for integration of  $i^o$  was implemented in MATLAB (MathWorks, Natick, MA, USA) and is described in detail in the Additional file 1: Supplementary Methods.

For statistics, paired, two-tailed  $t$  test was used to determine significance in comparisons between two groups in experiments where treatment and control were done within the same animal (i.e., lidocaine), and unpaired  $t$  test was used for comparisons between animals (i.e., reserpine, LPS). MATLAB's model fitting package was used for linear regression analysis and computation of  $r^2$  for stimulation intensity vs.  $Q^o$  in splenic stim and VNS experiments, and in  $Q^o$  vs. TNF a power model was used for regression instead due to the asymptote at  $Q^o=0$  causing non-linearity. Correlation between  $Q^o$  and TNF was tested with Spearman's ranked correlation coefficient due to the aforementioned non-linearity.  $P$  values less than 0.05 were considered significant. Means are reported with standard error. All calculations were done in MATLAB.

## Results

### A voltammetry signal in the spleen represents NE level

To define a physiological marker that assesses the release of NE in the spleen, a blood-filled organ, we first performed fast-scan cyclic voltammetry (FSCV) *in vitro* to establish the oxidation potential of NE in blood. We found that the oxidation potential of NE ( $E^o$ ) is  $0.72 \pm 0.05$  V in blood (at 3.3  $\mu\text{g/mL}$  NE concentration;  $n=3$ ), which is higher than what was found in PBS at  $0.57 \pm 0.02$  V (at 3.3  $\mu\text{g/mL}$  NE concentration;  $n=3$ ) (Fig. 1b; Additional file 1: Fig. S1a) in agreement with prior reports [25]. To determine  $E^o$  in the spleen and assess whether oxidation current ( $i^o$ ) tracks transient changes of NE concentration, we performed FSCV in the spleen during intravenous injections of NE using amounts estimated to produce peak concentrations of 0.01–0.5  $\mu\text{g/mL}$  in circulating blood. Injecting NE produces a voltammogram similar in shape to the *in vitro* in blood trace but with a higher  $E^o$  of  $0.88 \pm 0.02$  V ( $n=6$  experiments) (Additional file 1: Fig. S1a). During NE bolus injections,  $i^o$  rises and then returns to baseline, as opposed to saline injections, where  $i^o$  remains unchanged (Fig. 1c; Additional file 1: Fig. S1b).  $i^o$  starts increasing at approximately 0.02  $\mu\text{g}$  NE injection and increases further with increasing injected amounts of NE (Fig. 1c). To capture both the magnitude and the duration of the transient change in NE, we defined the "NE voltammetry signal" as the total oxidation charge ( $Q^o$ ), calculated as the area under the  $i^o$  trace, between the time of NE injection and the time at which  $i^o$  drops to pre-injection baseline level (Fig. 1c, black boxes).  $Q^o$  is linearly proportional to the estimated peak NE concentration in blood (Fig. 1d). From this data, we estimate the detection threshold of  $Q^o$  for NE to be 0.1  $\mu\text{g/mL}$  or less (Fig. 1d).

Together, these findings indicate that NE can be detected *in vivo* by voltammetry in the spleen, and that the NE voltammetry signal is proportional to the injected amount and the resulting (estimated) blood concentration of NE.

### NE voltammetry signal is responsive to bioelectronic activation of the splenic nerve

Electrical stimulation of the splenic nerve (SpNS) elicits its release of NE in the spleen [8]. To test whether the spleen voltammetry signal tracks NE release under these conditions, we performed FSCV in the spleen during SpNS (Fig. 1a). During SpNS,  $i^o$  rises and then settles back to baseline, as opposed to sham stimulation, where  $i^o$  remains unchanged (Fig. 2a). The shape of the voltammogram is similar to that recorded during the NE infusion experiments. The magnitude and duration of the  $i^o$  trace both increase with increasing

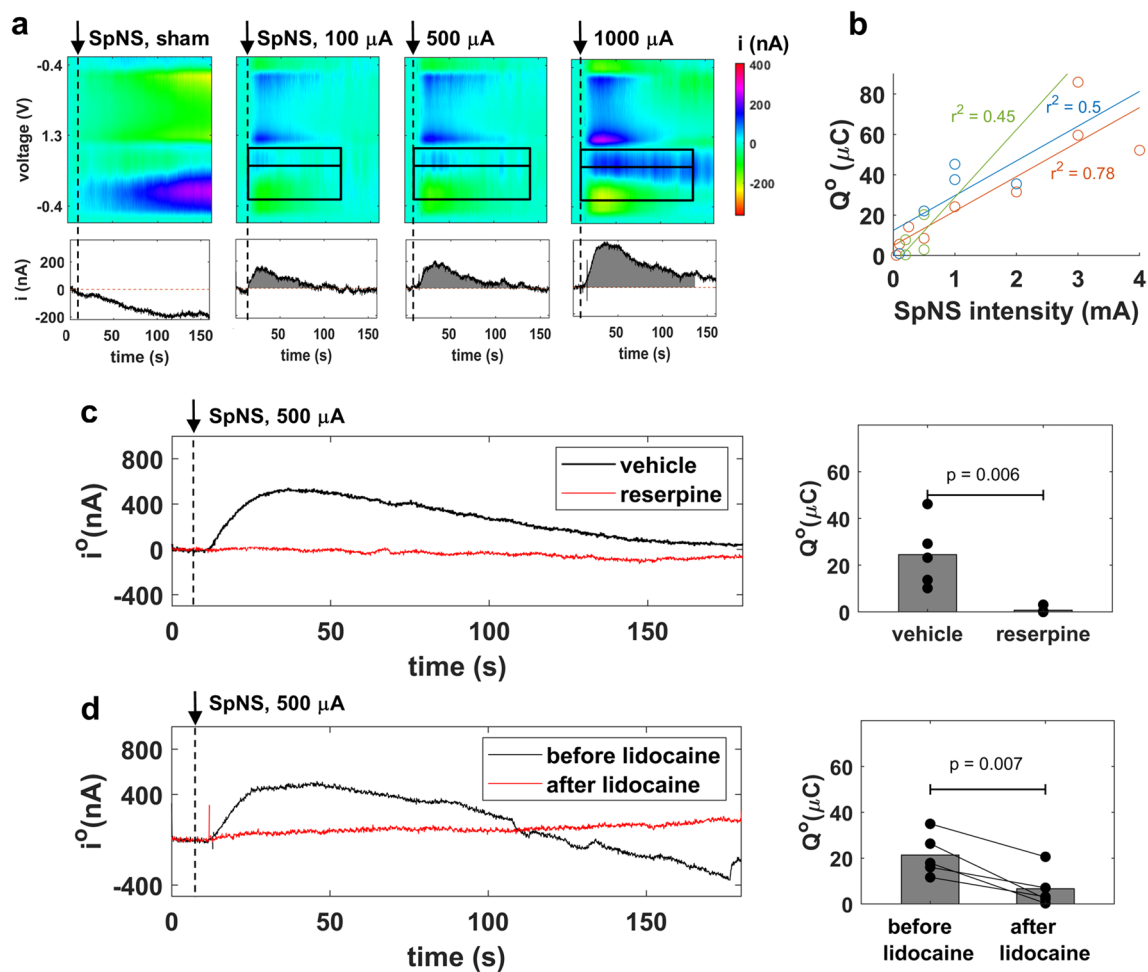


**Fig. 2** Activation of the splenic nerve by splenic nerve stimulation (SpNS) elicits a NE voltammetry signal in the spleen. **a** NE voltammetry signal elicited by SpNS (10 s duration, 500  $\mu\text{s}$  pulse width, 10 Hz pulsing frequency) or sham stimulation. Top and bottom panels similar to those of Fig. 1c. Dashed vertical line indicates the onset of SpNS. **b** Oxidation charge ( $Q^\circ$ ) vs. stimulation intensity in 3 animals, each represented by a different color; lines represent least square fits on data from each animal and  $r^2$  is the respective coefficients of determination. **c** Left panel: time course of NE peak oxidation current ( $i^\circ$ ) in response to SpNS, in reserpine- and vehicle-treated mice. Right panel:  $Q^\circ$  in response to SpNS in reserpine-treated vs. vehicle-treated animals ( $n=5$  in each group).  $p$  by unpaired  $t$  test. **d** Left panel: time course of  $i^\circ$  in response to SpNS recorded in the same animal before and after the topical application of lidocaine on the splenic nerve. Right panel:  $Q^\circ$  before and after lidocaine application, in 5 animals.  $p$  by paired  $t$  test

intensity of the electrical stimulus (Fig. 2a); expectedly,  $Q^\circ$  also increases with stimulus intensity (Fig. 2b).

To verify that the voltammetry signal elicited by SpNS is, at least partly, mediated by NE release, we performed FSCV during SpNS in animals treated with reserpine to deplete monoamines [4]. The NE voltammetry signal is absent in reserpine-treated animals; in contrast, it is evoked in vehicle-treated animals (Fig. 2c). To verify that the source of released NE is indeed the stimulated splenic nerve, SpNS was delivered before and after lidocaine, a local anesthetic agent blocking nerve depolarization, was directly applied on the splenic nerve. The NE voltammetry signal after

lidocaine application is significantly smaller compared to the signal before lidocaine (Fig. 2d).

Together, these findings indicate that the NE voltammetry signal in the spleen represents the release of NE in response to activation of the splenic nerve by SpNS.

#### NE voltammetry signal is responsive to bioelectronic activation of the efferent vagus and splanchnic nerves

Vagus nerve stimulation (VNS) elicits NE release in the spleen [30]. To determine whether the NE voltammetry signal is responsive to VNS, we performed FSCV in the spleen during cervical VNS. During VNS,  $i^\circ$  rises and then settles back to baseline, as opposed to sham

stimulation, where  $i^{\circ}$  remains unchanged (Fig. 3a); the magnitude of  $i^{\circ}$ , and of its derivative measure  $Q^{\circ}$ , are dose-responsive to VNS intensity (Fig. 3a, b).

To determine whether activation of afferent (sensory) or efferent (motor) vagus nerve is responsible for the observed NE voltammetry signal, VNS was delivered before and after dissection of the vagus nerve, above or below the level of stimulation (distal or proximal vagotomy, respectively). When VNS is delivered after distal vagotomy, the heart rate response disappears, and the NE voltammetry signal is diminished (Fig. 3c). In contrast, when VNS is delivered after proximal vagotomy, the breathing response disappears but the NE voltammetry signal is not affected (Fig. 3d). Likewise, selective activation of efferent vagal fibers by optogenetic VNS in ChAT-ChR mice, elicits the NE signal in the voltammogram. In contrast, selective activation of afferent vagal fibers, by optogenetic VNS in Vglut2-ChR mice, does not elicit a NE signal (Fig. 3e).

Splanchnic nerves provide sympathetic pre-ganglionic fibers to celiac-superior mesenteric ganglion neurons whose axons form the splenic nerve releasing NE to the spleen [31–34]. To determine whether activation of these preganglionic fibers results in a NE voltammetry signal in the spleen, we used fluorescence imaging in ChAT-tdTomato mice to isolate the splanchnic nerves (Additional file 1: Fig. S2) and delivered electrical splanchnic nerve stimulation using a cuff electrode. We found that stimulation of the splanchnic nerves elicits the NE voltammetry signal in the spleen (Fig. 3f). Splanchnic nerve stimulation at high pulsing frequency (30 Hz) consistently produces higher  $Q^{\circ}$  than at low pulsing frequency (2 Hz), indicating that the voltammetry signal is dose-responsive (Fig. 3f, g).

#### NE voltammetry signal maintains its shape across stimulation conditions

Voltammetric measurements can be affected by changes in the immediate environment of the working electrode, including temperature, chemical and biological factors, electrode surface area, and pH [35, 36]. In our studies, we performed FSCV in a large number of animals over several months, while regularly replacing the working electrode; in addition, FSCV was performed in combination with a variety of autonomic stimulation conditions and parameters. When overlaid, averaged raw voltammograms from all stimulation conditions have qualitatively consistent shapes (Fig. 4a). Values for NE oxidation potential were consistent among animals within same stimulation condition, and similar across different stimulation conditions (Fig. 4c). Peak oxidation currents ranged from 21.5 to 688.3 nA, while  $Q^{\circ}$  ranged from 2.3 to 121.7  $\mu\text{C}$  across all modalities (Fig. 4b, d, e). It is worth

noting that even though VNS parameters were relatively lower than SpNS, VNS produced lower  $Q^{\circ}$  and peak  $i^{\circ}$  (Fig. 4d, e) despite causing significant drops in heart rate and changes in breathing.

#### NE voltammetry signal during splenic nerve stimulation is predictive of subsequent TNF suppression in LPS endotoxemia

To determine whether the NE voltammetry signal in the spleen can assess the engagement of the anti-inflammatory neuroimmune pathway,  $Q^{\circ}$  was measured during splenic nerve stimulation (SpNS), followed by injection of LPS and, 90 min later, measurement of TNF from plasma samples (Fig. 5a). As expected from previous studies [8, 9, 12], we found that, overall, SpNS elicits suppression of TNF compared to sham stimulation (Fig. 5b). Importantly, we found that  $Q^{\circ}$  is inversely correlated with the degree of TNF suppression: smaller values of  $Q^{\circ}$  are associated with TNF suppression, whereas greater values of  $Q^{\circ}$  are associated with TNF values comparable to sham stimulation. As a result, about 40% of the variance in TNF values is explained by  $Q^{\circ}$  (Fig. 5c).

#### Discussion

Autonomic neurostimulation therapies aim to modulate a wide range of neural circuits, including those controlling inflammation, of which a significant component is the innervation of the spleen. Assessing the preclinical effectiveness of these therapies has relied on indirect measurements, i.e., levels of TNF after an LPS challenge, which are typically made hours after the stimulus has been delivered, oftentimes in terminal experiments [37]; such measurements cannot be used to assess engagement of the anti-inflammatory pathway in real time. Our work indicates that voltammetry in the spleen is an inexpensive and reproducible method to directly assess engagement of the anti-inflammatory pathway in response to autonomic neurostimulation. It also demonstrates, for the first time, a quantitative relationship between a physiological biomarker that is registered in real time, the NE voltammetry signal, and an immune-mediated response that is several steps downstream, the magnitude of TNF suppression in endotoxemia. Physiological markers of anti-inflammatory effectiveness could help in the implementation of precision autonomic neuromodulation therapies, by allowing calibration of stimulation parameters to maximize desired and minimize undesired, off-target, effects in individual subjects [17].

NE is the main neurotransmitter of the sympathetic nervous system, and the neurotransmitter released by fibers of the splenic nerve [38]. It belongs to a group of electrically active compounds termed catecholamines, which include epinephrine and dopamine [39]. Due to

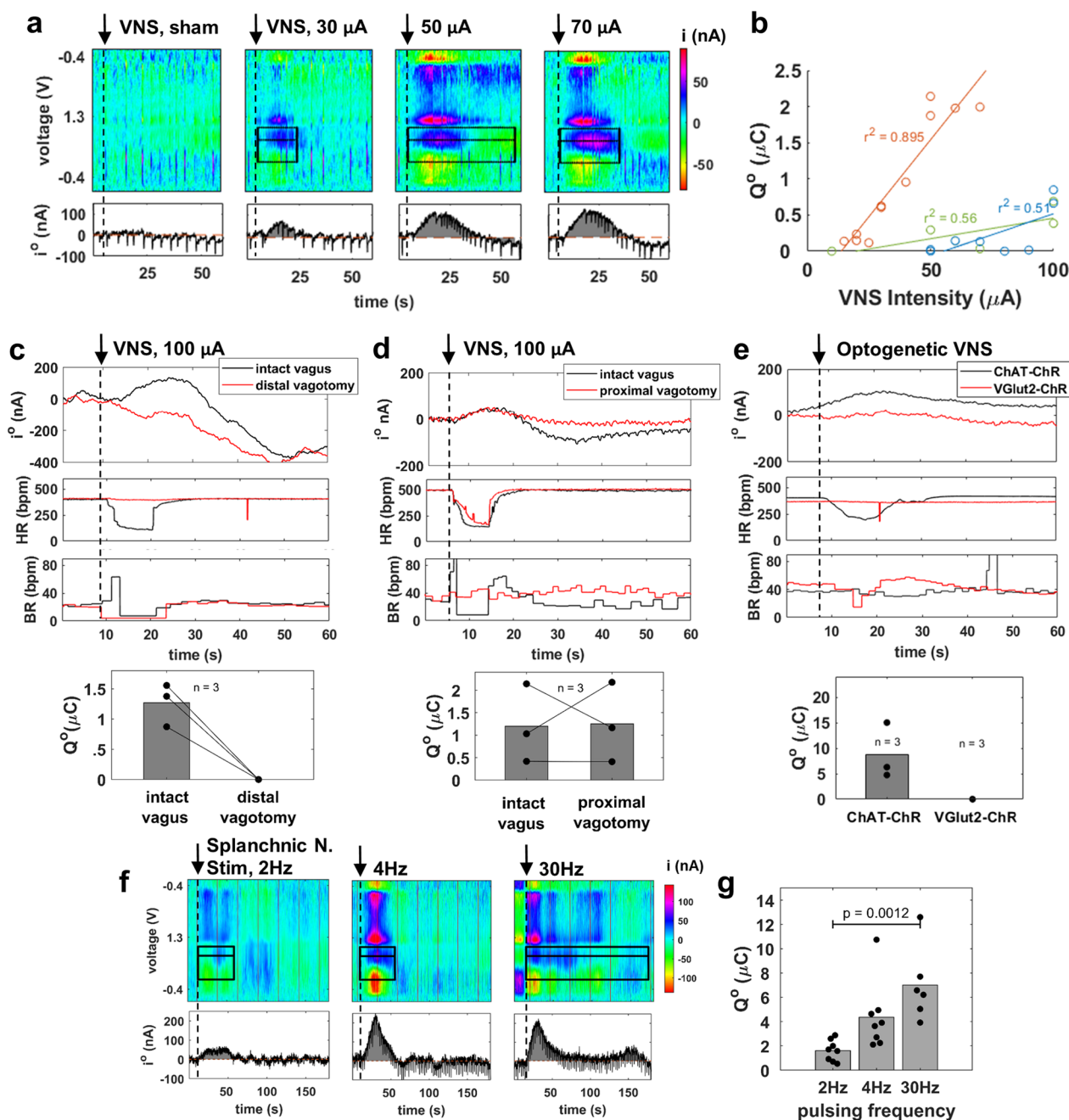


**Fig. 3** Stimulation of the efferent, but not afferent, vagus or of the splanchnic nerve elicits a NE voltammetry signal in the spleen. **a** Representative time-resolved voltammograms elicited by electrical left vagus nerve stimulation (VNS) (10–70  $\mu$ A intensity, 500  $\mu$ s pulse width, 10 Hz frequency, 10 s duration) or sham stimulation. Top and bottom panels are similar to those in Fig. 1c. The dashed vertical line denotes onset of VNS. **b** NE oxidation charge ( $Q^o$ ) in response to different VNS intensities in 3 animals; lines represent least square fits on data from each animal and  $r^2$  the respective coefficients of determination. **c** Time course of NE oxidation current ( $i^o$ ) elicited by VNS (top panel), associated heart rate and breathing rate responses (2 middle panels);  $Q^o$  values are shown in bottom panel, in 3 animals before and after distal vagotomy. **d** Same as **c**, but for proximal vagotomy. **e** Representative NE oxidation current trace elicited by optogenetic VNS in ChAT-ChR or in Vglut2-ChR mice (top panel), along with the associated heart rate and breathing rate responses (2 middle panels);  $Q^o$  values from 3 animals in each case are shown in bottom panel. **f** Representative time-resolved voltammograms elicited by electrical left splanchnic nerve stimulation (500  $\mu$ A intensity, 100  $\mu$ s pulse width, 2, 4, and 30 Hz frequency, 10 s duration). Top and bottom panels are similar to those in Fig. 1c. **g**  $Q^o$  values during splanchnic nerve stimulation using 2 (n=8), 4 (n=8), and 30 Hz (n=6) pulsing frequency.  $p$  by ANOVA with multiple comparisons

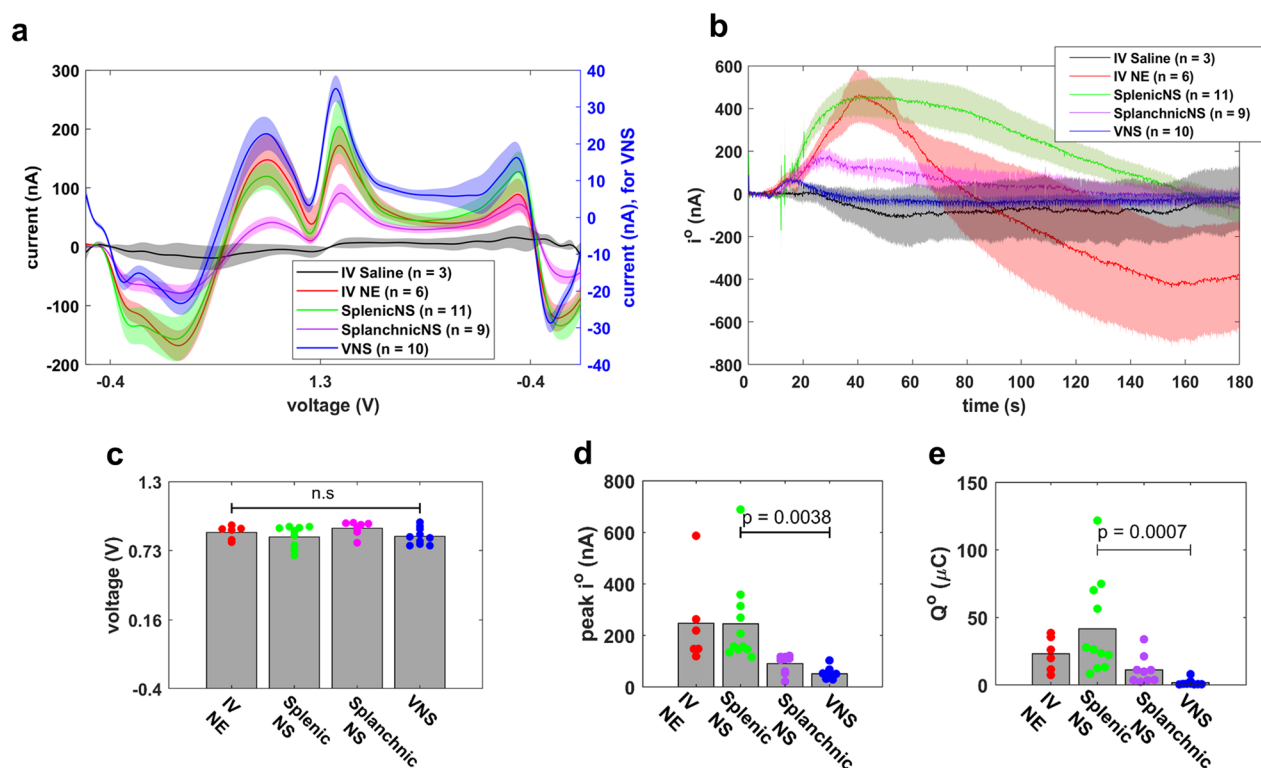


**Fig. 4** Average voltammetry NE signals in response to different stimulation conditions. **a** Average voltammograms during saline injections (3 animals), NE injections (6 animals), splenic nerve stimulation (11 animals), splanchnic nerve stimulation (9 animals) and vagus nerve stimulation (10 animals; plotted against ordinate on the right side of the plot). **b** Average time-course of peak oxidation currents over 3 min post-stimulation, during the same stimulation conditions. In **a** and **b**, shaded envelopes around solid traces represent SEM. **c** Oxidation potential during the same stimulation conditions, except saline injections. **d** Peak oxidation current during the same stimulation conditions. **e** Oxidation charge during the same stimulation conditions. *p* by ANOVA with multiple comparisons

its oxidation–reduction properties, changes in NE concentration can be detected by electrochemical methods, including cyclic voltammetry. Fast scan cyclic voltammetry (FSCV) can detect local changes in NE concentration in near real time, at low concentrations, and with increased spatial selectivity owing to its high cycling speed (400 V/s at 10 Hz) and the small scale of the working electrode [40]. When measuring in vitro in blood, we observed an  $E^{\circ}$  of approximately  $0.72 \pm 0.05$  V (Additional file 1: Fig. S1a), which agrees with previous reports [25]. When measuring from the spleen during intravenous NE injections,  $E^{\circ}$  is on average  $0.88 \text{ V} \pm 0.02$  (Additional file 1: Fig. S1a). One possible reason for the increase of  $E^{\circ}$  in tissue and blood compared to PBS ( $\sim 0.6$  V), is bio-fouling, a common phenomenon when electrochemical probes are implanted in biological tissues [41]. In addition, it is worth noting that the magnitude of the oxidation currents we recorded in vitro in blood were larger than previously recorded by Nicolai et al. [25]. This discrepancy can be explained by the larger working electrode used in our experiments ( $34 \mu\text{m}$  diameter  $\times$   $500 \mu\text{m}$  tip) compared to theirs ( $7 \mu\text{m} \times 100 \mu\text{m}$ ), which provides

a larger surface area for oxidation to occur, hence the higher currents [42].

During intravenous injection of NE,  $i^{\circ}$  rises within seconds and returns to baseline after several minutes. Furthermore,  $i^{\circ}$  and its derivative measure  $Q^{\circ}$  are dose-responsive with regard to the amount of injected NE (Fig. 1c, d). During saline injection or sham stimulation conditions  $i^{\circ}$  either did not change or it slowly drifted monotonically akin to a baseline drift (Fig. 1c; Additional file 1: Fig. S1b), but never exhibited transient changes seen during stimulation. Using intravenous injections of different amounts of NE, we found that  $0.01 \mu\text{g}/\text{mL}$  is the lowest (estimated) concentration that produces a voltammetry signal and at  $0.1 \mu\text{g}/\text{mL}$  a robust signal is always produced, indicating that detection threshold of our method is between  $0.01$  and  $0.1 \mu\text{g}/\text{mL}$ . To estimate the NE concentration in blood for a given amount of injected NE, we used the average blood volume of a mouse as the volume of distribution of NE; however, we did not directly measure the concentration of NE, this being a limitation of our study. Compared to previous reports, in which  $\sim 0.001$ – $0.01 \mu\text{g}/\text{mL}$  of NE were detected after

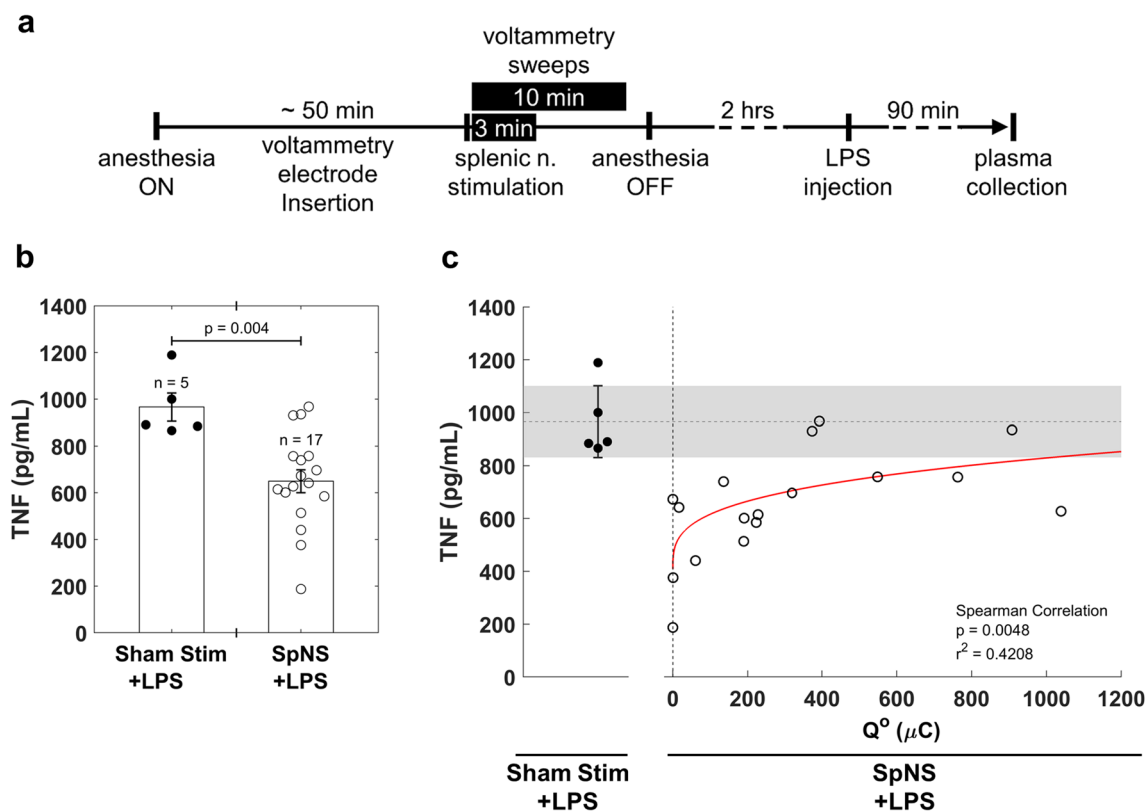


**Fig. 5** NE voltammetry signal during splenic nerve stimulation (SpNS) is predictive of subsequent TNF suppression in LPS endotoxemia. **a** Schematic representation of experimental timeline. Mice were anesthetized and instrumented with voltammetry electrodes. SpNS was delivered for 3 min (300–500  $\mu\text{A}$ , 500  $\mu\text{s}$ , 10 Hz) while performing voltammetry for 10 min to capture full signal. Lipopolysaccharide (LPS) was injected 2 h after SpNS and blood was collected 90 min post-LPS injection. **b** Plasma TNF levels 90 min post-LPS injection from animals that received SpNS compared with sham stimulated animals. Data presented as mean  $\pm$  SEM,  $p$  by unpaired  $t$  test. **c**  $Q^o$  values, measured during SpNS vs. levels of TNF in plasma, measured 90 min after LPS injection, in the same animals. Line represents second-order power fit;  $p$  by Spearman's correlation

neurostimulation [8, 9, 43, 44], the detection threshold of our system is relatively high. However, NE concentrations in previous reports were determined in processed blood samples using ELISA or mass spectrometry, where sample collection and processing to collect plasma or serum is typically done 5–10 min after stimulation. For that reason, NE concentrations at the time we perform voltammetry is likely greater, and above the detection threshold of the voltammetry method. Furthermore, the concentration of NE in the spleen parenchyma is likely higher than plasma levels, since only a small portion of it overflows to the circulation [45].

The motor arc of a well-studied neuroimmune pathway that controls inflammation starts with parasympathetic efferent vagal fibers and sympathetic efferent splanchnic nerve fibers synapsing on noradrenergic neurons of abdominal ganglia and continues with post-ganglionic noradrenergic fibers inside the splenic nerve [1, 3, 46–48]. Activation of this neuroimmune pathway via neurostimulation of the vagus, the splanchnic or the splenic nerve and its terminals results in activation of splenic

nerve fibers, release of NE in the spleen and subsequent suppression of manifestations of acute inflammatory responses [6, 8, 49–51]. Release of NE from splenic nerve fibers has been measured using biochemical assays measuring NE in splenic homogenates or inferred by recording splenic nerve activity after neurostimulation [4, 30]. However, such techniques cannot assess the real-time release dynamics of NE. In this study, we used voltammetry in the spleen to record a transient NE signal that is responsive to autonomic neurostimulation of several nerve targets that activate the anti-inflammatory neuro-immune pathway and suppress inflammation. For that reason, FSCV may be used in mechanistic studies of the regulation of inflammation by different components of the autonomic nervous system.

First, the NE voltammetry signal is responsive to stimulation of the splenic nerve (SpNS). The signal is proportional to stimulus intensity (Fig. 2a) and is suppressed by manipulations that block nerve activation by stimuli (Fig. 2d) or release of NE upon nerve activation (Fig. 2c). The NE signal appears within seconds after the

onset of SpNS and lasts from several seconds to several minutes, depending on stimulus intensity (Fig. 2a). This is consistent with previous studies in pigs and in human post-mortem specimens, in which splenic nerve evoked compound action potentials were found to increase with higher stimulation intensity or duration and were blocked by lidocaine [8, 9]. The amount of NE released into splenic venous outflow during SpNS was shown to increase with higher stimulation charge [9]. Furthermore, those studies showed that physiologic responses to SpNS, such as changes in blood pressure, last for more than a minute after stimulation [8, 9], resembling the kinetics of the elicited NE signal in our study. The NE signal in our study has a slower and longer time course than what is reported in voltammetry studies of catecholamine release in the brain, including NE and dopamine, which have indistinguishable voltammograms (e.g., [23, 52–54]). Due to the high density of neural processes in the brain, the voltammetry electrode has an intimate contact with nerve terminals and catecholamines are almost immediately detected. For example, Schluter et al. [54] recorded an evoked dopamine signal in the monkey brain of less than 100 ms latency lasting for 1 s, which was the duration of the stimulation train. In contrast, in the spleen, NE likely has to travel through the red pulp cords, where nerve fibers form a network [47], before sufficient concentration builds up at the voltammetry electrode. The majority of released NE in the spleen is cleared by reuptake via the high-affinity, low-capacity NE transporter (NET) [45, 55]. NET is inhibited by electrical stimulation [56], which could explain the relatively long duration of the NE voltammetry signal following SpNS (Fig. 2a).

Second, we found that the NE voltammetry signal is responsive to stimulation of the vagus nerve (Fig. 3a). This is consistent with previous observations that VNS exerts anti-inflammatory actions via a splenic nerve-dependent mechanism [4]. In addition, we found that the voltammetry signal is responsive to efferent but not afferent VNS (Fig. 3c–e). This is consistent with previous reports implicating efferent vagal fibers in relaying signals to the splenic nerve via the celiac–superior mesenteric ganglion complex [3, 7]. It is likely that afferent vagal fibers may also contribute to the anti-inflammatory effect, via delayed engagement of multi-synaptic, vagal-sympathetic and vagal–vagal reflexes [32, 33, 57]; however, the lack of a temporally precise volley of action potentials reaching the spleen in response to afferent VNS may be responsible for the lack of a clear NE voltammetry signal. The voltammetry signal after efferent VNS has consistently lower magnitude than that after splenic nerve stimulation, even after stimulation at relatively high intensities that produce a significant drop in heart rate and change in breathing (Fig. 4b, d–e). A possible explanation may

be that VNS results in eliciting action potentials only on a subset of postganglionic splenic nerve fibers or in activating those fibers at a sub-maximal degree. This implies that VNS at relatively low intensities might elicit release of NE at levels below the limit of detection of the voltammetry method. Studies that demonstrated anti-inflammatory actions of VNS at levels below those that induce a reduction in heart rate support this notion [50].

Third, the NE voltammetry signal is responsive to direct stimulation of the splanchnic nerve (Fig. 3f). To demonstrate this, we used a ChAT–tdTomato mouse strain to visualize and isolate the celiac–superior mesenteric ganglion complex and the associated splanchnic nerve. Although this ganglion and the splanchnic nerve have been isolated under direct vision [33, 58], we report here, for the first time, that the use of fluorescence microscopy improves yield and accuracy. The finding that splanchnic nerve stimulation elicits a NE signal in the spleen is consistent with reports that implicate splanchnic nerve activity in the anti-inflammatory effect of VNS [31–34]. For example, administering VNS with the splanchnic nerve sectioned abolishes the TNF-lowering effect of stimulation in a model of LPS endotoxemia [33].

Notably, the magnitude of the NE voltammetry signal varies across animals, regardless of the stimulated nerve. This variability may arise because of differences in electrode placement directly affecting the number of activated nerve fibers, even at identical stimulus intensities. This underlines the need for using quantifiable markers of target engagement for calibration of the dose of bioelectronic therapies [17, 21]. Another source of signal variability may lie with the voltammetry technique itself. It is likely that the location of the voltammetry electrode in the spleen relative to nerve endings influences the signal. The noradrenergic innervation of the spleen has a mesh-like structure and is most dense towards the center of the organ [46, 47]. Although the working length of the voltammetry electrode was the same in all of our experiments (500  $\mu\text{m}$ ), the exact insertion depth into the spleen likely varied, affecting which anatomical compartment of the spleen was sampled. This source of variability is a limitation of single-electrode cyclic voltammetry; it will have to be quantified in future studies with multiple voltammetry electrodes, capturing NE voltammetry signals from several sites in the spleen.

Previous studies of LPS endotoxemia report considerable variability in the degree of TNF suppression in response to VNS or SpNS [12, 37, 57]. Consistently, we find that the same intensity of SpNS produces a wide range of TNF suppression responses in animals injected with LPS (Fig. 5b); for example, out of 17 stimulated animals, at least 3 have TNF values similar to those of sham-stimulated controls. The magnitude of the NE

voltammetry signal during SpNS explains about 40% of this variability. Traditionally, these non-responding experiments are usually attributed to inadequate stimulation or engagement of the splenic nerve. However, we find here that TNF suppression is more likely to occur when stimulation results in relatively small  $Q^o$  values but is often minimal with greater values of  $Q^o$  (Fig. 5). Given NE's established anti-inflammatory effects, it would be expected that higher levels would produce a larger TNF-lowering response. In contrast, we report an inverse relationship that has not been previously described, and it may explain some of the non-responding experiments reported in the literature. Monocytes/macrophages are known to express both  $\alpha$ - and  $\beta$ -adrenergic receptors (ARs);  $\alpha$ -ARs are typically associated with mediating pro-inflammatory signaling and bind NE with high affinity at low concentrations, whereas  $\beta$ -ARs mediate anti-inflammatory effects and only bind NE at high concentrations [59–62]. Upon SpNS, NE concentration is highest at nerve terminals, where it is released, and lower away from nerve terminals [60]. Therefore, the location of immune cells relative to nerve terminals may affect the anti-inflammatory response to SpNS. It is possible to consider that relatively small NE release may only affect ChAT<sup>+</sup> T cells that lie close to nerve terminals by binding  $\beta_2$ -ARs and causing acetylcholine release, which then acts on macrophages to inhibit TNF release. In contrast, greater NE release may result in monocytes/macrophages located further away, in the red pulp of the spleen, to be exposed to small but not zero concentrations of NE, binding high-affinity  $\alpha$ -ARs and favoring TNF release [47, 60]. In fact, in a similar model of endotoxemia, one study found that co-treating animals with both  $\alpha$ - and  $\beta$ -AR agonists resulted in TNF suppression similar to that in vehicle treated animals, while treating with an  $\alpha$ - or  $\beta$ -AR agonist alone increased or decreased TNF, respectively [62]. Furthermore, large stimulus intensities or pulsing frequencies might induce the release of co-transmitters, such as NPY and ATP, that are also immune-modulators and might negate the NE effect [60, 63]. Therefore, it is conceivable that non-responders to neurostimulation, reported frequently in previous studies, could be in fact animals that were under- or over-stimulated. In our study, which produced a range of  $Q^o$  values, animals with high  $Q^o$  values showed smaller TNF suppression (Fig. 5C). In a study by Brinkman et al. [12], most of the animals receiving splenic nerve stimulation had TNF values close to those of the sham-stimulated group (~6000 pg/mL vs. ~7500 pg/mL, respectively). The results from our study, which used similar stimulation parameters, suggest that in the Brinkman et al. study it is likely that in a subset of animals that showed smaller TNF suppression,  $Q^o$  may have been similarly high. These

findings underscore the potential usefulness of FSCV as a tool to calibrate stimulation dose and optimize intensity and other stimulation parameters to achieve a predictable anti-inflammatory response within and across subjects. Although a recent study in pigs suggests changes in splenic artery flow as a marker of effective splenic nerve stimulation [8], this approach is indirect and does not reflect the actual NE content in the spleen. Changes in blood flow in the splenic artery could be mediated by direct effects of stimulation on vessel-innervating fibers [64], and not necessarily reflect activation of nerve fibers that terminate in the spleen. Furthermore, the mere engagement of splenic nerve fibers may not be a good predictor of the anti-inflammatory response, since more NE release may have less of an anti-inflammatory effect as our data suggest. For those reasons, when setting up a stimulating device, the use of a direct, real-time measure of NE rather than aiming for maximum release may be beneficial. Future studies should determine whether the NE threshold of detection can be used as a reference value to gauge stimulation parameters akin to the heart rate threshold (HRT) used to calibrate VNS parameters [27, 51]. Splenic NE threshold could be used to establish treatment protocols or adjust stimulation dose overtime.

The FSCV method has several limitations. First, the method is invasive, as it requires puncture and repair of the spleen, which might alter the splenic response and introduce an additional source of variability. This variability is likely to be minor, as the range of TNF responses we observed is similar to previously reported data using the same LPS and concentration [50]. Second, our configuration has a relatively high threshold for detection of NE, which may limit its use in some neuromodulation therapies, for example, auricular or low-level VNS [65–67]. Third, due to variations in the voltammetry electrode placement, measurement of  $Q^o$  has low spatial resolution and differences in signal magnitude may partially represent variations in electrode location relative to intrinsic nerves or splenic blood supply. Finally, FSCV using our methodology cannot distinguish between different catecholamines (e.g., NE and dopamine) due to their similar chemical structures [68]. However, since dopamine is typically co-released with NE in very small amounts [69], its contribution to the signal is likely minimal.

Recent advances in voltammetry electrode fabrication allow integration onto highly flexible biocompatible materials and its implantation into various organs to record catecholamine transients. For example, the use of platinum wires allowed the detection of real-time NE release in a beating heart overcoming the fragile nature of carbon fibers [26]. Furthermore, Li et al. developed a flexible and stretchable multichannel interface integrated on a graphene–elastomer composite, which they

used to measure monoamine transients chronically in the brain and gut [70]. These technological advances, along with progress in the processing and analysis of voltammograms, may facilitate the development of implanted devices that continuously monitor catecholamine release in the spleen as part of integrated autonomic stimulation systems [71]. One potential implementation could include a voltammetry electrode on a catheter advanced to the splenic hilum via the splenic vein, where it measures NE in blood exiting the spleen. This procedure could be used during the clinical programming of a stimulation implant to determine parameters that elicit detectable levels of NE while avoiding relatively high levels. Closed-loop stimulation devices, with a voltammetry electrode permanently implanted to provide feedback on the engagement of the anti-inflammatory circuit, could make use of this technology. However, significant technological barriers must be overcome to achieve this level of integration. This includes advances in electrode design to allow for a stable, long-term voltammetry electrode that can resist biofouling and provide a strong signal in a highly dynamic environment.

## Conclusion

Tools to monitor the anti-inflammatory effectiveness of neurostimulation are needed to calibrate and adjust neurostimulation dose and develop precision bioelectronic therapies. FSCV in the spleen detects in real-time NE release in response to autonomic neurostimulation, which correlates with engagement of the anti-inflammatory neuroimmune pathway. Several obstacles remain to be overcome for this approach to be widely adopted, including the development of stable, high-fidelity implantable electrodes and minimally invasive procedures. With these advances, FSCV can be used pre-clinically to resolve neural circuits activated by existing neurostimulation approaches, to identify new targets for autonomic neuromodulation, and to optimize stimulation parameters with regard to the anti-inflammatory effect. Ultimately, with further development and validation, FSCV could be used clinically to provide a continuous readout associated with anti-inflammatory therapeutic efficacy.

## Abbreviations

FSCV	Fast scan cyclic voltammetry
NE	Norepinephrine
PBS	Phosphate buffered saline
SpNS	Splenic nerve stimulation
$E^{\circ}$	Oxidation potential
$i^{\circ}$	Oxidation current
$Q^{\circ}$	Total oxidation charge
VNS	Vagus nerve stimulation
IV	Intravenous
LPS	Lipopolysaccharide

ChAT	Choline acyl transferase
Vglut2	Vesicular glutamate transporter 2
ChR	Channel rhodopsin
AR	Adrenergic receptor
TNF	Tumor necrosis factor alpha
NET	Norepinephrine transporter

## Supplementary Information

The online version contains supplementary material available at <https://doi.org/10.1186/s12974-023-02902-x>.

**Additional file 1: Figure S1.** (a) Average oxidation potential ( $E^{\circ}$ ) of NE in vitro (in PBS and in blood, 3.3  $\mu\text{g}/\text{mL}$ ,  $n = 3$  in each condition) and in vivo (in live spleen, 0.5  $\mu\text{g}/\text{mL}$ ,  $n = 6$ ).  $p$  by ANOVA with multiple comparisons. (b) Averaged and time-resolved voltammograms from experiments in 3 animals in each of which NE (approximately 100–200  $\mu\text{L}$  of 10  $\mu\text{g}/\text{mL}$  NE) or saline (equivalent volume) was administered as IV bolus; also shown are the respective  $i^{\circ}$  traces, for both NE and saline injections, demonstrating how the algorithm identifies temporal boundaries of the NE signal. (c)  $Q^{\circ}$  values calculated using the temporal boundaries shown in (b). **Figure S2.** Left celiac–superior mesenteric (CSM) ganglion complex is identified using fluorescence microscopy in ChAT–tdTomato mice (ChAT+ tissue appears in red). The splanchnic nerve is isolated and cuffed with a bipolar stimulating electrode.

## Acknowledgements

The authors thank Kip Ludwig and James Trevantham from University of Wisconsin-Madison for their helpful discussions, and Jason Wong from the Feinstein Institutes for assembling the optical cuff used in optogenetic stimulation experiments.

## Author contributions

ITM, MG conceived, designed, and performed experiments, analyzed data, interpreted data, and wrote the paper. NJ conceived and designed experiments. SPP designed experiments. TD, CS interpreted the data and wrote the paper. VAP and YAA wrote the paper. SZ conceived and designed experiments, analyzed data, interpreted data, wrote the paper. All authors approved the final version.

## Funding

This research was conducted using departmental funds from the Feinstein Institutes for Medical Research.

## Availability of data and materials

The analysis algorithms, along with all of the raw data can be found here: <https://github.com/mgerber000/SpleenFSCV>.

## Declarations

### Ethics approval and consent to participate

Animal experiments were conducted according to the US National Institutes of Health guidelines and were approved by the Institutional Animal Care and Use Committee (IACUC) of the Feinstein Institute for Medical Research (Protocol # 2019-010).

### Consent for publication

Not applicable.

### Competing interests

The authors declare that they have no competing interests.

### Author details

<sup>1</sup>Institute of Bioelectronic Medicine, The Feinstein Institutes for Medical Research, Manhasset, NY, USA. <sup>2</sup>Donald & Barbara Zucker School of Medicine at Hofstra/Northwell, Hempstead, NY, USA. <sup>3</sup>Department of Physiology and Biophysics, Case Western Reserve University, Cleveland, OH, USA. <sup>4</sup>Elmezzzi Graduate School of Molecular Medicine, Manhasset, NY, USA.

Received: 30 March 2023 Accepted: 22 September 2023  
Published online: 17 October 2023

## References

- Tracey KJ. Reflex control of immunity. *Nat Rev Immunol.* 2009;9(6):418–28.
- Kenney MJ, Ganta CK. Autonomic nervous system and immune system interactions. *Compr Physiol.* 2014;4(3):1177–200.
- Pavlov VA, Chavan SS, Tracey KJ. Molecular and functional neuroscience in immunity. *Annu Rev Immunol.* 2018;36:783–812.
- Rosas-Ballina M, Ochani M, Parrish WR, Ochani K, Harris YT, Huston JM, et al. Splenic nerve is required for cholinergic antiinflammatory pathway control of TNF in endotoxemia. *Proc Natl Acad Sci USA.* 2008;105(31):11008–13.
- Gigliotti JC, Huang L, Ye H, Bajwa A, Chattrabhuti K, Lee S, et al. Ultrasound prevents renal ischemia-reperfusion injury by stimulating the splenic cholinergic anti-inflammatory pathway. *J Am Soc Nephrol.* 2013;24(9):1451–60.
- Zachs DP, Offutt SJ, Graham RS, Kim Y, Mueller J, Auger JL, et al. Noninvasive ultrasound stimulation of the spleen to treat inflammatory arthritis. *Nat Commun.* 2019;10(1):951.
- Kressel AM, Tsaava T, Levine YA, Chang EH, Addorisio ME, Chang Q, et al. Identification of a brainstem locus that inhibits tumor necrosis factor. *Proc Natl Acad Sci USA.* 2020;117(47):29803–10.
- Donega M, Fjordbakk CT, Kirk J, Sokal DM, Gupta I, Hunsberger GE, et al. Human-relevant near-organ neuromodulation of the immune system via the splenic nerve. *Proc Natl Acad Sci USA.* 2021;118(20):e2025428118.
- Sokal DM, McSloy A, Donega M, Kirk J, Colas RA, Dolezalova N, et al. Splenic nerve neuromodulation reduces inflammation and promotes resolution in chronically implanted pigs. *Front Immunol.* 2021;12: 649786.
- Tanaka S, Abe C, Abbott SGB, Zheng S, Yamaoka Y, Lipsey JE, et al. Vagus nerve stimulation activates two distinct neuroimmune circuits converging in the spleen to protect mice from kidney injury. *Proc Natl Acad Sci USA.* 2021;118(12):e2021758118.
- Ahmed U, Graf JF, Daytz A, Yaipen O, Mughrabi I, Jayaprakash N, et al. Ultrasound neuromodulation of the spleen has time-dependent anti-inflammatory effect in a pneumonia model. *Front Immunol.* 2022;13: 892086.
- Brinkman DJ, Simon T, Ten Hove AS, Zafeiropoulou K, Welting O, van Hamersveld PHP, et al. Electrical stimulation of the splenic nerve bundle ameliorates dextran sulfate sodium-induced colitis in mice. *J Neuroinflammation.* 2022;19(1):155.
- Birmingham K, Gradinaru V, Anikeeva P, Grill WM, Prikov V, McLaughlin B, et al. Bioelectronic medicines: a research roadmap. *Nat Rev Drug Discov.* 2014;13(6):399–400.
- Koopman FA, Chavan SS, Miljko S, Grazio S, Sokolovic S, Schuurman PR, et al. Vagus nerve stimulation inhibits cytokine production and attenuates disease severity in rheumatoid arthritis. *Proc Natl Acad Sci USA.* 2016;113(29):8284–9.
- Kaniusas E, Kampusch S, Tittgemeyer M, Panetsos F, Gines RF, Papa M, et al. Current directions in the auricular vagus nerve stimulation II—an engineering perspective. *Front Neurosci.* 2019;13:772.
- Kaniusas E, Kampusch S, Tittgemeyer M, Panetsos F, Gines RF, Papa M, et al. Current directions in the auricular vagus nerve stimulation I—a physiological perspective. *Front Neurosci.* 2019;13:854.
- Ahmed U, Chang YC, Zafeiropoulos S, Nassrallah Z, Miller L, Zanos S. Strategies for precision vagus neuromodulation. *Bioelectron Med.* 2022;8(1):9.
- Ben-Menachem E. Vagus nerve stimulation, side effects, and long-term safety. *J Clin Neurophysiol.* 2001;18(5):415–8.
- Mulders DM, de Vos CC, Vosman I, van Putten MJ. The effect of vagus nerve stimulation on cardiorespiratory parameters during rest and exercise. *Seizure.* 2015;33:24–8.
- Goyal RK, Chaudhury A. Physiology of normal esophageal motility. *J Clin Gastroenterol.* 2008;42(5):610–9.
- Chang YC, Cracchiolo M, Ahmed U, Mughrabi I, Gabalski A, Daytz A, et al. Quantitative estimation of nerve fiber engagement by vagus nerve stimulation using physiological markers. *Brain Stimul.* 2020;13(6):1617–30.
- Abbas A, Mughrabi IT, Zanos S, editors. Laryngeal electromyography to estimate a—fiber engagement by vagal stimuli in mice. In: 2021 10th International IEEE/EMBS Conference on Neural Engineering (NER); 2021 4–6 May 2021.
- Schwerdt HN, Shimazu H, Amemori KI, Amemori S, Tierney PL, Gibson DJ, et al. Long-term dopamine neurochemical monitoring in primates. *Proc Natl Acad Sci USA.* 2017;114(50):13260–5.
- Puthongkham P, Venton BJ. Recent advances in fast-scan cyclic voltammetry. *Analyst.* 2020;145(4):1087–102.
- Nicolai EN, Trevathan JK, Ross EK, Lujan JL, Blaha CD, Bennet KE, et al. Detection of norepinephrine in whole blood via fast scan cyclic voltammetry. *IEEE Int Symp Med Meas Appl.* 2017;2017:111–6.
- Chan SA, Vaseghi M, Kluge N, Shivkumar K, Ardell JL, Smith C. Fast in vivo detection of myocardial norepinephrine levels in the beating porcine heart. *Am J Physiol Heart Circ Physiol.* 2020;318(5):H1091–9.
- Ahmed U, Chang YC, Lopez MF, Wong J, Datta-Chaudhuri T, Rieth L, et al. Implant- and anesthesia-related factors affecting cardiopulmonary threshold intensities for vagus nerve stimulation. *J Neural Eng.* 2021;18(4).
- Meunier CJ, Roberts JG, McCarty GS, Sombers LA. Background signal as an in situ predictor of dopamine oxidation potential: improving interpretation of fast-scan cyclic voltammetry data. *ACS Chem Neurosci.* 2017;8(2):411–9.
- Harkness J, Wagner J. Biology and husbandry. The biology and medicine of rabbits and rodents. 1989:372.
- Rosas-Ballina M, Olofsson PS, Ochani M, Valdes-Ferrer SI, Levine YA, Reardon C, et al. Acetylcholine-synthesizing T cells relay neural signals in a vagus nerve circuit. *Science.* 2011;334(6052):98–101.
- Martelli D, Farmer DG, Yao ST. The splanchnic anti-inflammatory pathway: could it be the efferent arm of the inflammatory reflex? *Exp Physiol.* 2016;101(10):1245–52.
- Abe C, Inoue T, Inglis MA, Viar KE, Huang L, Ye H, et al. C1 neurons mediate a stress-induced anti-inflammatory reflex in mice. *Nat Neurosci.* 2017;20(5):700–7.
- Komegae EN, Farmer DGS, Brooks VL, McKinley MJ, McAllen RM, Martelli D. Vagal afferent activation suppresses systemic inflammation via the splanchnic anti-inflammatory pathway. *Brain Behav Immun.* 2018;73:441–9.
- McKinley MJ, Martelli D, Trevizan-Bau P, McAllen RM. Divergent splanchnic sympathetic efferent nerve pathways regulate interleukin-10 and tumour necrosis factor- $\alpha$  responses to endotoxaemia. *J Physiol.* 2022;600(20):4521–36.
- Jones SR, Mickelson GE, Collins LB, Kawagoe KT, Wightman RM. Interference by pH and Ca<sup>2+</sup> ions during measurements of catecholamine release in slices of rat amygdala with fast-scan cyclic voltammetry. *J Neurosci Methods.* 1994;52(1):1–10.
- Roberts JG, Sombers LA. Fast-scan cyclic voltammetry: chemical sensing in the brain and beyond. *Anal Chem.* 2018;90(1):490–504. <https://doi.org/10.1021/acs.analchem.7b04732>
- Caravaca AS, Gallina AL, Tarnawski L, Tracey KJ, Pavlov VA, Levine YA, et al. An effective method for acute vagus nerve stimulation in experimental inflammation. *Front Neurosci.* 2019;13:877.
- Karemaker JM. An introduction into autonomic nervous function. *Physiol Meas.* 2017;38(5):R89–118.
- Molinoff PB, Axelrod J. Biochemistry of catecholamines. *Annu Rev Biochem.* 1971;40:465–500.
- Rodeberg NT, Sandberg SG, Johnson JA, Phillips PE, Wightman RM. Hitchhiker's guide to voltammetry: acute and chronic electrodes for in vivo fast-scan cyclic voltammetry. *ACS Chem Neurosci.* 2017;8(2):221–34.
- Seaton BT, Hill DF, Cowen SL, Heien ML. Mitigating the effects of electrode biofouling-induced impedance for improved long-term electrochemical measurements in vivo. *Anal Chem.* 2020;92(9):6334–40.
- Chadchankar H, Yavich L. Characterization of a 32  $\mu$ m diameter carbon fiber electrode for in vivo fast-scan cyclic voltammetry. *J Neurosci Methods.* 2012;211(2):218–26.
- Torres-Rosas R, Yehia G, Pena G, Mishra P, del Rocio T-B, Moreno-Eutimio MA, et al. Dopamine mediates vagal modulation of the immune system by electroacupuncture. *Nat Med.* 2014;20(3):291–5.
- Liu S, Wang Z, Su Y, Qi L, Yang W, Fu M, et al. A neuroanatomical basis for electroacupuncture to drive the vagal-adrenal axis. *Nature.* 2021;598(7882):641–5.
- Dearnaley DP, Geffen LB. Effect of nerve stimulation on the noradrenaline content of the spleen. *Proc R Soc Lond B Biol Sci.* 1966;166(1004):303–15.

46. Ding X, Wang H, Qian X, Han X, Yang L, Cao Y, et al. Panicle-shaped sympathetic architecture in the spleen parenchyma modulates antibacterial innate immunity. *Cell Rep*. 2019;27(13):3799–807e3.
47. Hu D, Al-Shalan HAM, Shi Z, Wang P, Wu Y, Nicholls PK, et al. Distribution of nerve fibers and nerve-immune cell association in mouse spleen revealed by immunofluorescent staining. *Sci Rep*. 2020;10(1):9850.
48. Pavlov VA, Tracey KJ. The cholinergic anti-inflammatory pathway. *Brain Behav Immun*. 2005;19(6):493–9.
49. Borovikova LV, Ivanova S, Zhang M, Yang H, Botchkina GI, Watkins LR, et al. Vagus nerve stimulation attenuates the systemic inflammatory response to endotoxin. *Nature*. 2000;405(6785):458–62.
50. Huffman WJ, Subramaniam S, Rodriguez RM, Wetsel WC, Grill WM, Terrando N. Modulation of neuroinflammation and memory dysfunction using percutaneous vagus nerve stimulation in mice. *Brain Stimul*. 2019;12(1):19–29.
51. Mughrabi IT, Hickman J, Jayaprakash N, Thompson D, Ahmed U, Papadopyannis ES, et al. Development and characterization of a chronic implant mouse model for vagus nerve stimulation. *Elife*. 2021;10.
52. Park J, Takmakov P, Wightman RM. In vivo comparison of norepinephrine and dopamine release in rat brain by simultaneous measurements with fast-scan cyclic voltammetry. *J Neurochem*. 2011;119(5):932–44.
53. Clark JJ, Sandberg SG, Wanat MJ, Gan JO, Horne EA, Hart AS, et al. Chronic microsensors for longitudinal, subsecond dopamine detection in behaving animals. *Nat Methods*. 2010;7(2):126–9.
54. Schluter EW, Mitz AR, Cheer JF, Aeverbeck BB. Real-time dopamine measurement in awake monkeys. *PLoS ONE*. 2014;9(6): e98692.
55. Gasser PJ. Organic cation transporters in brain catecholamine homeostasis. In: Daws LC, editor. *Organic cation transporters in the central nervous system*. Cham: Springer International Publishing; 2021. p. 187–97.
56. Cao LL, Marshall JM, Fabritz L, Brain KL. Resting cardiac sympathetic firing frequencies suppress terminal norepinephrine transporter uptake. *Auton Neurosci*. 2021;232: 102794.
57. Murray K, Rude KM, Sladek J, Reardon C. Divergence of neuroimmune circuits activated by afferent and efferent vagal nerve stimulation in the regulation of inflammation. *J Physiol*. 2021;599(7):2075–84.
58. Mohanta SK, Peng L, Li Y, Lu S, Sun T, Carnevale L, et al. Neuroimmune cardiovascular interfaces control atherosclerosis. *Nature*. 2022;605(7908):152–9.
59. Chhatar S, Lal G. Role of adrenergic receptor signalling in neuroimmune communication. *Curr Res Immunol*. 2021;2:202–17.
60. Pongratz G, Straub RH. The sympathetic nervous response in inflammation. *Arthritis Res Ther*. 2014;16(6):504.
61. Ahlquist RP. A study of the adrenotropic receptors. *Am J Physiol*. 1948;153(3):586–600.
62. Szelenyi J, Kiss JP, Vizi ES. Differential involvement of sympathetic nervous system and immune system in the modulation of TNF- $\alpha$  production by  $\alpha$ 2- and  $\beta$ -adrenoceptors in mice. *J Neuroimmunol*. 2000;103(1):34–40.
63. Todorov LD, Mihaylova-Todorova ST, Bjur RA, Westfall DP. Differential cotransmission in sympathetic nerves: role of frequency of stimulation and prejunctional autoreceptors. *J Pharmacol Exp Ther*. 1999;290(1):241–6.
64. Ren LM, Nakane T, Chiba S. Characteristics of the responses of isolated and perfused canine splenic arteries to vasoactive substances and to periarterially electrical stimulation. *Jpn J Pharmacol*. 1994;64(1):19–25.
65. Go YY, Ju WM, Lee CM, Chae SW, Song JJ. Different transcutaneous auricular vagus nerve stimulation parameters modulate the anti-inflammatory effects on lipopolysaccharide-induced acute inflammation in mice. *Biomedicines*. 2022;10(2):247.
66. Zhao YX, He W, Jing XH, Liu JL, Rong PJ, Ben H, et al. Transcutaneous auricular vagus nerve stimulation protects endotoxemic rat from lipopolysaccharide-induced inflammation. *Evid Based Complement Alternat Med*. 2012;2012: 627023.
67. Hong GS, Zillekens A, Schneiker B, Pantelis D, de Jonge WJ, Schaefer N, et al. Non-invasive transcutaneous auricular vagus nerve stimulation prevents postoperative ileus and endotoxemia in mice. *Neurogastroenterol Motil*. 2019;31(3): e13501.
68. Schmidt KT, McElligott ZA. Dissecting the catecholamines: how new approaches will facilitate the distinction between noradrenergic and dopaminergic systems. *ACS Chem Neurosci*. 2019;10(4):1872–4.
69. Goldstein DS, Holmes C. Neuronal source of plasma dopamine. *Clin Chem*. 2008;54(11):1864–71.
70. Li J, Liu Y, Yuan L, Zhang B, Bishop ES, Wang K, et al. A tissue-like neurotransmitter sensor for the brain and gut. *Nature*. 2022;606(7912):94–101.
71. Datta-Chaudhuri T. Closed-loop neuromodulation will increase the utility of mouse models in Bioelectronic Medicine. *Bioelectron Med*. 2021;7(1):10.

## Publisher's Note

Springer Nature remains neutral with regard to jurisdictional claims in published maps and institutional affiliations.

Ready to submit your research? Choose BMC and benefit from:

- fast, convenient online submission
- thorough peer review by experienced researchers in your field
- rapid publication on acceptance
- support for research data, including large and complex data types
- gold Open Access which fosters wider collaboration and increased citations
- maximum visibility for your research: over 100M website views per year

At BMC, research is always in progress.

Learn more [biomedcentral.com/submissions](https://biomedcentral.com/submissions)

